

Roller-Quadrotor: A Novel Hybrid Terrestrial/Aerial Quadrotor with Unicycle-Driven and Rotor-Assisted Turning

Zhi Zheng^{1,2}, Jin Wang^{†1,2}, Yuze Wu³, Qifeng Cai^{1,2}, Huan Yu^{1,2},
Ruimin Zhang³, Jie Tu^{1,2}, Jun Meng^{2,4}, Guodong Lu^{1,2}, and Fei Gao³

Abstract— Roller-Quadrotor is a novel hybrid terrestrial and aerial quadrotor that combines the elevated maneuverability of the quadrotor with the lengthy endurance of the ground vehicle. This work presents the design, modeling, and experimental validation of Roller-Quadrotor. Flying is achieved through a quadrotor configuration, and four actuators providing thrust. Rolling is supported by unicycle-driven and rotor-assisted turning structure. During terrestrial locomotion, the vehicle needs to overcome rolling and turning resistance, thus saving energy compared to flight mode. This work overcomes the challenging problems of general rotorcraft, reduces energy consumption and allows to pass through special terrain, such as narrow gaps. It also solves the obstacle avoidance challenge faced by terrestrial robots by flying. We design the models and controllers for the vehicle. The experiment results show that it can switch between aerial and terrestrial locomotion, and be able to safely pass through a narrow gap half the size of its diameter. Besides, it is capable of rolling a distance approximately 3.8 times as much as flying or operating about 42.2 times as lengthy as flying. These results demonstrate the feasibility and effectiveness of the structure and control in rolling through special terrain and energy saving.

I. INTRODUCTION

In recent years, unmanned aerial vehicles (UAVs) have been increasingly used in various fields such as military, exploration and rescue applications[1]. These applications pose challenges on UAVs in terms of energy consumption[2] and passing through special terrain, particularly narrow gaps[3]. To encounter the above difficulties, advanced technologies must be developed to improve the endurance and terrain adaptability of UAVs. This could significantly expand the range of applications for UAVs. Unfortunately, it is hard to address multiple challenges simultaneously by optimizing a traditional UAV.

For energy consumption, Zhang et al. propose an innovative solution using quadrotor pitching to provide a forward thrust, as inputs to control the rolling of the passive wheels on

¹The State Key Laboratory of Fluid Power and Mechatronic Systems, School of Mechanical Engineering, and the Engineering Research Center for Design Engineering and Digital Twin of Zhejiang Province, School of Mechanical Engineering, Zhejiang University, Hangzhou 310027, China.

²Robotics Institute of Zhejiang University, Hangzhou 310027, China.

³The State Key Laboratory of Industrial Control Technology, College of Control Science and Engineering, Zhejiang University, Hangzhou 310027, China, and Huzhou Institute of Zhejiang University, Huzhou 313000, China.

⁴Center for Data Mining and Systems Biology, College of Electrical Engineering, Zhejiang University, Hangzhou 310027, China.

Email: {z.z, dwjcom}@zju.edu.cn

†Corresponding author: Jin Wang.

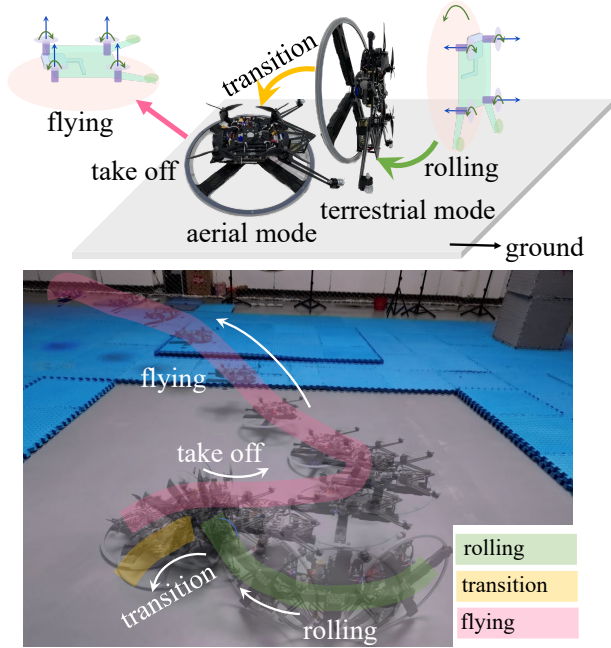


Fig. 1. The vehicle rolls on the ground, transitions, and finally takes off and flies.

the ground and fly over obstacles[4][5][6]. A similar idea is adopted in Kalantari et al. and Dudley et al.'s work[7][8][9]. However, when the aircraft approaches the ground, the airflow around the rotors may become turbulent due to the influence of the ground effect (Wing-In-Ground effect / Wing-In-Surface-Effect)[10]. This may cause changes in lift and drag that directly affect the precision of the motion control. This brings serious problems to the control model and controller design. Besides, adding wheels perpendicular to the UAV frame plane significantly increases the size and weight of the UAV, reduces the maneuverability. In conclusion, although the scheme based on quadrotor and differential wheel can reduce energy consumption, it has adverse effects. Therefore, it is difficult to achieve large-scale application.

Many efforts have been made to improve terrain adaptability. In application scenarios such as inspection and exploration, vehicles may need to pass through narrow gaps and passages such as square ventilation ducts and urban sewer pipes. This is a trail for UAVs applications.

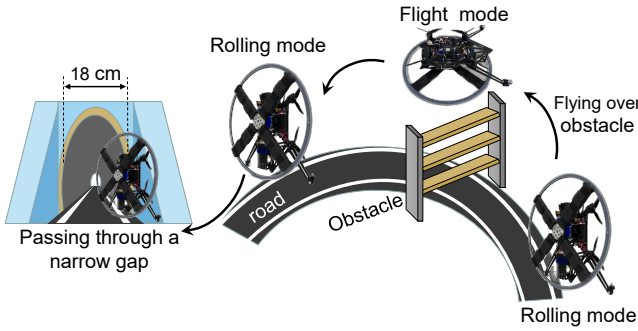


Fig. 2. Schematic diagram of Roller-Quadrotor rolling on road, flying over obstacle and passing through narrow gap.

Falanga et al. propose foldable mechanical designs for the airframe[11][12][13]. A morphing quadrotor is proposed to allow its robot to fold the structure and reduce its span for passing narrow apertures[14]. Bucki et al. proposed a bird-inspired robot, it has passive joints that can shrink its footprint by temporarily reducing propulsion commands to squeeze through a narrow gap[15]. However, due to the existence of moving parts, the folding mechanism introduces additional degrees of freedom, which makes the system model deeply nonlinear. In addition, extreme vibration is inevitable during the flight of the UAV, which will considerably affect the reliability and lifetime of the deformation mechanism, and affect the safety of the UAV. Besides, error accumulation is inevitable during deformation, leading to the inaccurate motion control of the UAV. In conclusion, folding mechanisms are useful for passing through narrow gaps, but it has many disadvantages that make it difficult to apply in practice.

In short, there is no single technology that can solve multiple challenges at the same time. To address these issues, we propose a nonfolding quadrotor with a driving wheel called Roller-Quadrotor. This is a novel hybrid terrestrial and aerial quadrotor. Based on quadrotor, the addition of an unicycle-driven and rotor-assisted turning structure enables terrestrial locomotion of the vehicle, and to roll through narrow gaps. Compared to traditional UAVs, the proposed Roller-Quadrotor has the advantage of low energy consumption.

We design models and controllers for vehicle rolling and transition in aerial and terrestrial locomotion. These are improvements based on planar unicycle motion model and first-order inverted pendulum model. The vehicle has been tested in real environment to demonstrate its functions and performance, and compared with other vehicles to show its innovation and feasibility.

As for energy consumption, it can roll a distance about 3.8 times as much as flying or operate nearly 42.2 times as lengthy as flying. Compared with another hybrid terrestrial and aerial quadrotor[7][8], it still increases the operating time in rolling mode under the same vehicle mass. In terms of terrain adaptability, especially rolling through narrow gaps, the vehicle has an excellent aspect ratio (about 3) in hybrid terrestrial and aerial quadrotors, with a diameter of 36 cm

and a width of 12 cm in rolling mode. This allows it to roll through narrow gaps half of its diameter which is narrower than others.

The contribution of the proposed Roller-Quadrotor is summarized as follows:

- Propose a novel hybrid terrestrial and aerial quadrotor with an unicycle-driven and rotor-assisted turning structure. This structure enables the vehicle to roll energy-savingly under terrestrial locomotion, and improve terrain adaptability, especially rolling through narrow gaps.
- Design models and controllers for vehicle rolling and transition between aerial and terrestrial locomotion which are on the basis of optimizing the motion model of the plane unicycle and the first-order inverted pendulum model.
- Conduct plenty of experiments, and the results show that it can roll a distance nearly 3.8 times as much as flying or operate about 42.2 times as long as flying, and can safely pass through a gap half of its diameter.

Overall, the proposed Roller-Quadrotor is a significant innovation in the field of hybrid terrestrial and aerial quadrotors, improving the endurance and terrain adaptability and offering new capabilities and potential applications.

II. MECHATRONIC SYSTEM DESIGN

This section first discusses the system architecture and components of Roller-Quadrotor mechatronic system, and then introduces the drive and transmission system design.

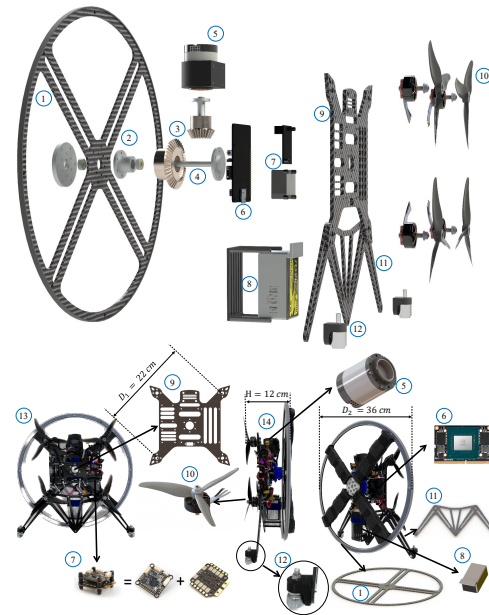


Fig. 3. The detailed composition of Roller-Quadrotor. The serial numbers represent (1) four-spoke wheel, (2) bearing, (3) bevel gears, (4) shaft, (5) servomotor, (6) onboard computer, (7) flight controller and electronic speed controller (ESC), (8) battery, (9) quadrotor frame, (10) rotors and 5-inch three-blade propellers, (11) frame support plate, (12) horn gimbals, (13) the top view of the actual vehicle, (14) lateral view of the actual vehicle.

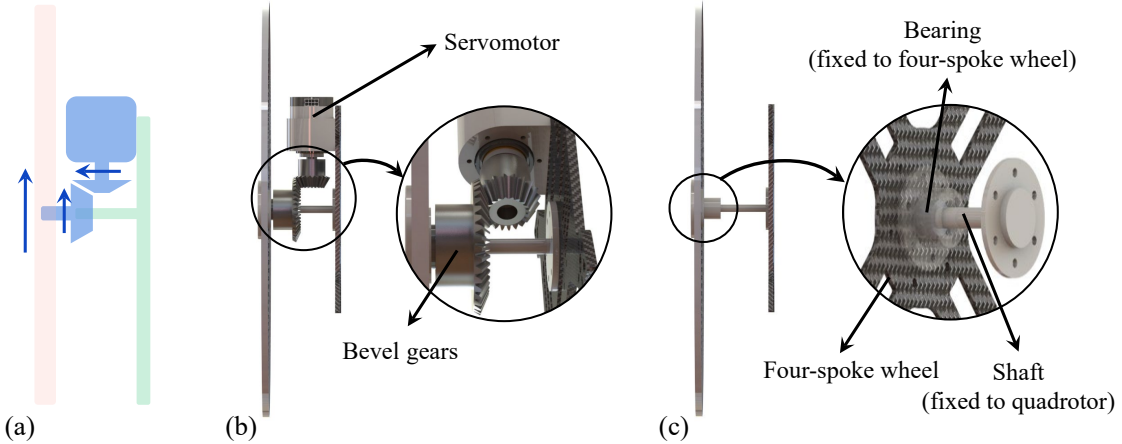


Fig. 4. Roller-Quadrotor's drive and transmission system design of rolling mode.

A. System Architecture and Components

In the flight mode, the top view of the actual vehicle is shown in Fig. 3 (13). The main body is an asymmetrical design with an X-shaped frame with a 22 cm axle diameter. (see Fig. 3 (9)). This vehicle uses TMOTOR F60 PRO 2550KV rotors and 5-inch three-blade propellers to output thrust (see Fig. 3 (10)). The flight controller and electronic speed controller (ESC) use the Holybro Kakute H7 v1 and Tekko32 Metal 4 in 1 65A ESC STACK (see Fig. 3 (7)).

In order to run the rolling mode at low energy consumption and pass through narrow gaps, we design a four-spoke wheel (see Fig. 3 (1)) as the main body of its rolling mode. The wheel has a diameter of 36 cm and is wrapped with a white rubber ring on the outer ring to increase the frictional force. The wheel is driven by a servomotor (see Fig. 3 (5)) attached to the shaft of the frame through a transmission system. The frame is connected to a frame support plate (see Fig. 3 (11)) at the end of which two horn gimbals (see Fig. 3 (12)) are mounted. The horn gimbals are in contact with the ground to counterbalance the reverse torque output of the motor during rolling and provide a mechanical limit to ensure the stability of the frame pitch angle during rolling.

The system is powered by a 2000 mAh 4S battery (see Fig. 3 (8)), which is mounted on the different side of the servomotor to help stabilize the body's center of gravity. We choose NVIDIA Jetson Xavier (see Fig. 3 (6)) as the on-board computer, which is connected to the flight controller for rotor thrust and reversing control via the serial port. NVIDIA Jetson Xavier also connects to the servomotor for torque and speed control via the CAN bus.

For strength considerations, we use carbon fiber as the main structural material of Roller-Quadrotor, including the frame (see Fig. 3 (9)), the frame support plate (see Fig. 3 (11)), and the four-spoke wheel (see Fig. 3 (1)). We also wrapped a sponge strip around the four-spoke wheel to cushion the impact when switching to flight mode.

In summary, Roller-Quadrotor is designed to achieve low power consumption and to pass through narrow space using

its rolling mode.

B. Drive and Transmission System Design

When rolling mode is activated, the servomotor generates torque to produce rolling rotation around the initial yaw axis. This torque is then transmitted through bevel gears (see Fig. 4(b) and (c)) with a transmission ratio of $i = 2$. The four-spoke wheel is mounted on the frame's fixed shaft and connected to the frame by bearing (see Fig. 4(d)).

At the same time, the differential thrust generated by the four rotors (see Fig. 8) provides yaw torque. This distinct combination of ground rolling and differential thrust provides the vehicle with a more flexible and efficient ground motion capability than previous rolling vehicles. In addition, this approach significantly reduces the energy consumption and is more suitable for rolling through narrow gaps.

In summary, the vehicle's rolling mode uses a servomotor to generate rolling torque, which is transmitted to the four-spoke wheel via bevel gears. The differential thrust generated by the four rotors provides the yaw torque, allowing the vehicle to achieve a more versatile ground motion capability such as rolling through narrow gap, while reducing energy consumption.

III. MODELING AND CONTROL

In this section, we will discuss the various configurations of Roller-Quadrotor and the corresponding modeling for each configuration in sequential order.

A. Rotor Thrus/Torque Model

Defined the thrust and torque generated by the i th ($i \in 1, 2, 3, 4$) rotor as F_i and τ_i . For accurate control of vehicles in non-flying modes, the thrust and torque generated by each rotor F_i is found as a function of rotational speed ω_i as

$$\begin{cases} F_i = \kappa_f * (\omega_i)^2 \\ \tau_i = \kappa_m * (\omega_i)^2 \end{cases} \quad (1)$$

It can be seen from Eq.1 that the thrust F_i depends on parameters coefficient of thrust namely κ_f , and the torque τ_i depends on parameters coefficient of torque namely κ_m .

In the non-flight mode of the vehicle, the thrust F_i and torque τ_i generated by the rotors are not used for hovering or flying. We expect a relatively slight thrust F_i from the rotor, even we do not need to control the torque τ_i , in which case the angular speed ω_i is linear to square of thrust F_i and torque τ_i . Angular speed ω_i can still be maintained relatively nicely and it is acceptable to consider κ_f and κ_m as a constant.

The vehicle gravity and rotor angular speed ω_i in hover are measured. κ_f is obtained by Eq.1, and κ_m is obtained by torque measuring instrument.

The flight controller can control the angular speed ω_i by communicating with ESC through dshot protocol. We use a quadratic function to model the angular speed ω_i versus dshot U_d curve as:

$$\omega_i = p_1 * U_d^2 + p_2 * U_d + p_3 \quad (2)$$

It can be seen from Eq.2 that the speed ω_i depends on several parameters, namely p_1 , p_2 , p_3 .

Find the angular speed ω_i and dshot U_d data in the log of the flight controller and fit the data to get the coefficients p_1 , p_2 , p_3 using Eq.2. Therefore, we can control the rotor angular velocity ω_i output by inputting the desired dshot values U_d corresponding to the four rotors. In this way we can get the final thrust F_i and torque κ_m outputs.

B. Wheel Torque/Force Model

For accurate control of torque τ_w and force F_w of wheel in non-flying modes, according to the mechanical drive structure, we can calculate the output on the wheel by:

$$\begin{cases} P_s = \tau_s * \omega_s \\ \omega_w = \omega_s / i \\ \nu_w = \omega_w * R_w \\ \tau_w = \tau_s / i \\ F_w = \tau_w / R_w \end{cases} \quad (3)$$

where P_s is the servomotor output power, R_w is the radius of the wheel and i is transmission ratio. R_w and i are constants.

It can be seen from Eq.3, by controlling the angular velocity ω_s and torque τ_s output of the servomotor, we are able to accurately control the angular velocity ω_w , linear velocity ν_w , torque τ_w and force F_w of the wheel.

C. Flight Model

In this part, we will describe Roller-Quadrotor during take-off and flying, using four rotors for lift and propulsion. In this configuration, Roller-Quadrotor can maneuver in three-dimensional space, hover in place, and move in any direction with great agility and speed.

When the four-spoke wheel of Roller-Quadrotor touches a flat surface and the quadrotor is configured horizontally, the vehicle is in flight mode. The dynamics state of Roller-Quadrotor in flight is similar to a conventional quadrotor.

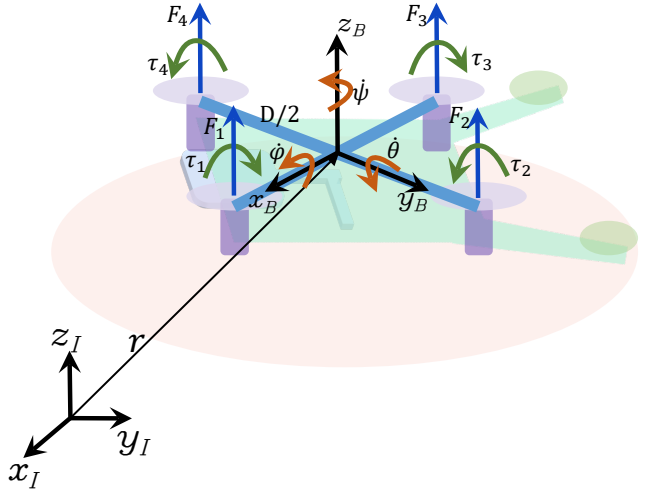


Fig. 5. The rigid body diagram of the quadrotor[18].

Next, we will introduce the essential dynamic model of the quadrotor. When the vehicle is in flight mode, the quadrotor is driven by four rotors. Defined the thrust and torque generated by the i th ($i \in 1, 2, 3, 4$) rotor as F_i and τ_i . In body fixed frame \mathcal{B} , we can define four control inputs U_i composed of F_i and τ_i as follows[18]:

$$\begin{cases} U_1 = F_1 + F_2 + F_3 + F_4 \\ U_2 = (F_2 - F_4)D/2 \\ U_3 = (F_3 - F_1)D/2 \\ U_4 = \tau_2 + \tau_4 - \tau_1 - \tau_3 \end{cases} \quad (4)$$

where D_q is diagonal propeller distance of the quadrotor.

Thus, the essential dynamic model[19] of the vehicle in flight mode can be expressed as:

$$\begin{cases} m\ddot{\mathbf{r}} = \mathbf{R}_{\mathcal{I}}^{\mathcal{B}}(U_1 \mathbf{Z}_B) - mg \mathbf{Z}_I \\ \mathbf{I}\ddot{\mathbf{q}} = [U_2, U_3, U_4]^T - S(\mathbf{G}\mathbf{q})\mathbf{I}(\mathbf{G}\mathbf{q}) \end{cases} \quad (5)$$

where $\mathbf{r} = [x, y, z]^T$ is the position of the center of mass in the inertial coordinates I , $\mathbf{q} = [\phi, \theta, \psi]^T$ is the attitude, G represents the affine from the attitude angles to the angular velocities, m and I are the mass and moments of inertia of the quadrotor, g is the gravity constant, $\mathbf{R}_{\mathcal{I}}^{\mathcal{B}}$ is the transform matrix between the inertial frame I and the body-fixed frame \mathcal{B} as defined in Fig. 5, and $S(\cdot)$ is the skew matrix representation of the corresponding vector.

In summary, with Eq.1 and Eq.2, by inputting the direction and dshot U_d values of the four rotors, we can obtain U_i , $i \in 1, 2, 3, 4$ in Eq.4, and then use Eq.5 to model the flight mode.

D. Transition Model

In this part, we will discuss the transition, which is a key feature of Roller-Quadrotor. Transition from flying to rolling involves reconfiguring the quadrotor into a rolling platform where the rotors are used to assist turning rather than lift. This mode allows Roller-Quadrotor to move efficiently over flat surfaces and traverse rough terrain.

And transition from rolling to flying is where Roller-Quadrotor reconfigures back into a quadrotor for aerial maneuvering. This transition allows Roller-Quadrotor to overcome obstacles and navigate to locations inaccessible on the ground, such as steep edges and rooftops.

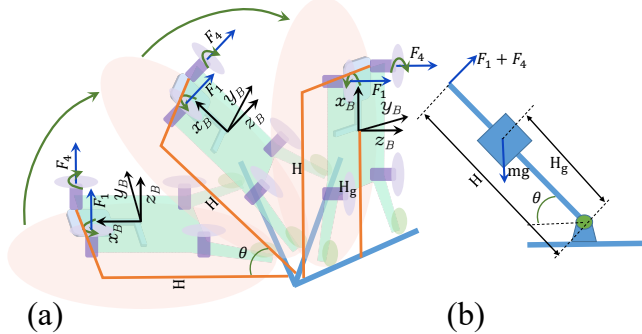


Fig. 6. Dynamic model of transition.

As shown in Fig. 6, the quadrotor is driven by two rotors when the vehicle is in transition. On the basis of optimizing the first-order inverted pendulum model[16], we establish the control model and controller of transition between aerial and terrestrial locomotion.(see Fig. 6(b)):

$$\begin{cases} ml^2\ddot{\theta} + mlg \cos(\theta) = \tau \\ l = H_g \\ \tau = (F_1 + F_4)H \end{cases} \quad (6)$$

$$\tau = \alpha\tau' + \beta \quad (7)$$

when $\alpha = ml^2$, $\beta = mlg \cos(\theta)$, the system is equivalent to $\ddot{\theta} = \ddot{\theta}$. The controller output is:

$$\tau'_1 = \ddot{\theta}_d + k_v(\dot{\theta}_d - \dot{\theta}) + k_p(\theta_d - \theta) \quad (8)$$

The control block diagram is as follows:

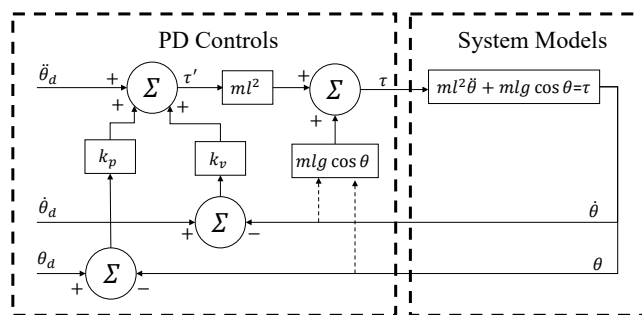


Fig. 7. Control block diagram of transition.

E. Terrestrial Locomotion Model

In this part, we will focus on the terrestrial locomotion of Roller-Quadrotor, which uses a rolling motion to move forward, backward, and turning. This mode of operation is particularly useful for navigating through confined spaces and obstacles, as well as for performing tasks that require precise positioning and manipulation.

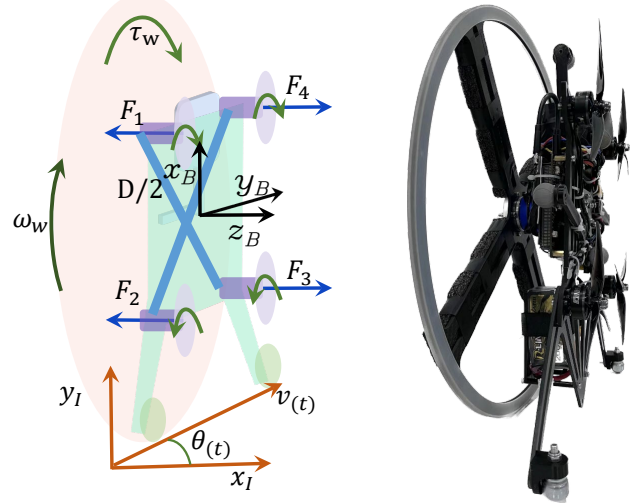


Fig. 8. Dynamic model of terrestrial locomotion.

We developed a model and controller for vehicle rolling based on the optimization of the motion model of the planar unicycle model[17]. As shown in Fig. 8, when the vehicle is in rolling mode, the quadrotor is driven by one servomotor and four rotors.

Defined the thrust generated by the i th($i \in 1, 2, 3, 4$) rotor as F_i , the angular velocity, linear velocity, torque and force of the wheel as ω_w , v_w , τ_w and F_w , which we can directly control using Eq.1, 2 and 3.

Defined the position of vehicle at moment t are $p_x(t)$, $p_y(t)$, $p_z(t)$, and $p_z(t) = 0$. Defined the linear velocity and yaw of vehicle at moment t are $v_{(t)}$ and $\theta_{(t)}$.

$$\tau = I\beta = I \frac{d\omega}{dt} = (F_1 + F_2 - F_3 - F_4)\sqrt{2}D/4 \quad (9)$$

Based on this, we model the state-space as:

$$x_1(t) = p_x(t), x_2(t) = p_y(t), x_3(t) = v_{(t)}, x_4(t) = \theta_{(t)} \quad (10)$$

$$\vec{x}_{(t)} = [p_x(t), p_y(t), v_{(t)}, \theta_{(t)}] \quad (11)$$

In body fixed frame β , We can define two control inputs U_i as follows:

$$U_1 = \alpha_{(t)}, U_2 = \omega_{(t)} \quad (12)$$

$$\vec{u}(t) = \begin{bmatrix} u_1(t) \\ u_2(t) \end{bmatrix} = \begin{bmatrix} \alpha(t) \\ \omega(t) \end{bmatrix} \quad (13)$$

where $\alpha(t)$ is linear acceleration and $\omega(t)$ is angular velocity of yaw.

We establish the state space equation:

$$\frac{d\vec{x}(t)}{dt} = \begin{bmatrix} \nu_{(t)} \cos \theta_{(t)} \\ \nu_{(t)} \sin \theta_{(t)} \\ 0 \\ 0 \end{bmatrix} + \begin{bmatrix} 0 \\ 0 \\ \alpha(t) \\ \omega(t) \end{bmatrix} = f(\vec{x}(t), \vec{u}(t)) \quad (14)$$

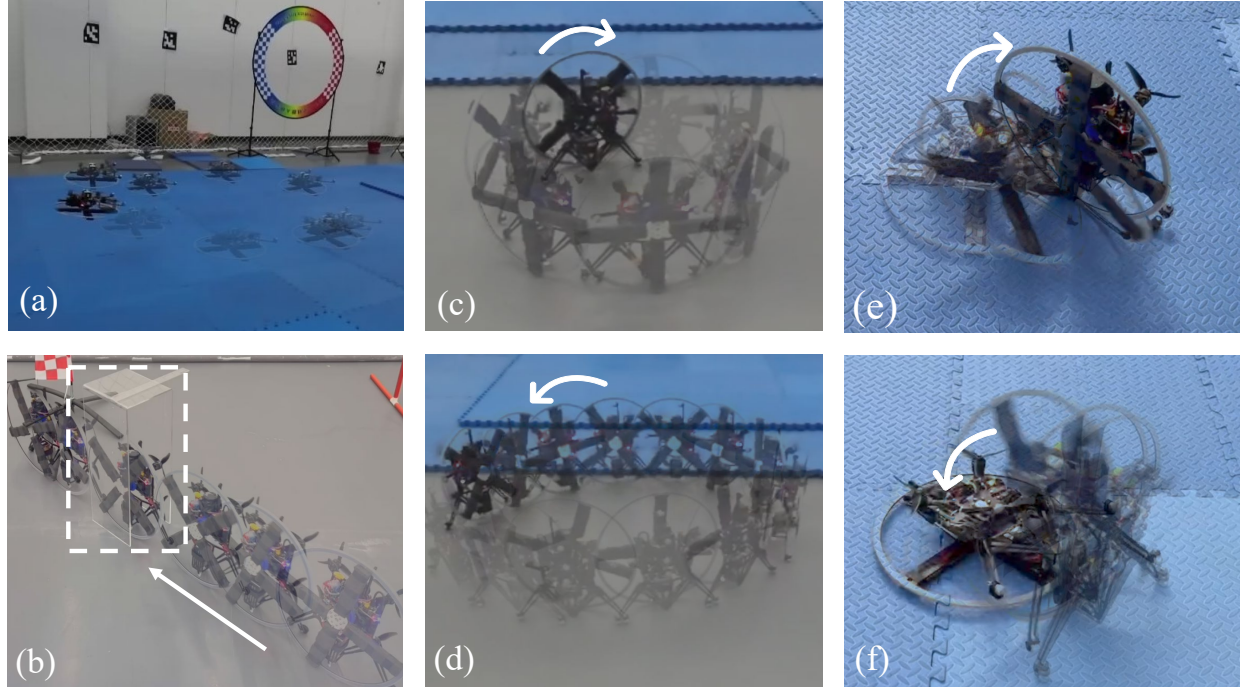


Fig. 9. (a) Residual image from experiment of hand-flying. (b) Residual image from experiment of passing through a narrow gap of 18 cm. (c) Residual image from clockwise rolling circle experiments. (d) Residual image from counterclockwise rolling circle experiments. (e) Residual image of transition from flying to rolling. (f) Residual image of transition from rolling to flying.

When giving the desired trajectory:

$$\begin{bmatrix} x_{1d}[k] \\ x_{2d}[k] \end{bmatrix} = \begin{bmatrix} p_{xd}[k] \\ p_{yd}[k] \end{bmatrix} \quad (15)$$

$$J = \|\vec{x}[N] - \vec{x}_d[N]\|_S^2 + \sum_{k=1}^{N-1} \left(\|\vec{x}_{[k]} - \vec{x}_d[k]\|_Q^2 + \|\vec{u}_{(k)}\|_R^2 \right) \quad (16)$$

where J is performance measure, S, Q, R are weight coefficient matrix.

Optimize the U^* . Make sure that J is minimized.

IV. EXPERIMENTAL VALIDATION

In this section, flight mode, rolling mode, and modal transitions were implemented based on the built model and controller. Finally, Roller-Quadrotor successfully passes through narrow gaps by rolling in a narrow gap of 18 cm.

A. Experimental Setup

For indoor experiments, an $18\text{ m} \times 9\text{ m} \times 5\text{ m}$ motion capture gym with 22 Vicon cameras is used as the experimental site. The state estimation of the quadrotor is given by an EKF of the pose from the Vicon cameras and the IMU data from an APM autopilot.

B. Experiments of Taking Off and Flying

Experiment 1: We conduct hand-flying experiments in Stabilize mode in the APM flight controller environment, and the maximum tracking error was 0.0555 rad and 0.0440 rad during 30 seconds of flight when the expected roll and pitch were within 0.3 rad , respectively (see Fig. 9 (a) and Fig. 10 (a)). Experiment 1 shows that the vehicle is capable of flight.

rad during 30 seconds of flight when the expected roll and pitch were within 0.3 rad , respectively (see Fig. 9 (a) and Fig. 10 (a)). Experiment 1 shows that the vehicle is capable of flight.

C. Experiments of Transition

Experiment 2 and 3: We conduct plenty of experiments on modal transition from flying to rolling and from rolling to flying on a foam floor (see Fig. 9 (e) and (f)). Unfortunately, the success rate of Experiment 2 is not satisfactory and the process of Experiment 3 is still not smooth and seamless enough, though modal transitions were done successfully.

D. Experiments of Terrestrial Locomotion

1) *Pass Through a Narrow Gap:* Experiment 4: We build a gap/tunnel model made from acrylic with dimensions of $20\text{ cm} \times 18\text{ cm} \times 50\text{ cm}$. And the opening of the model is 18 cm (see the white part in Fig. 9 (b)). We try to conduct the experiments in rolling mode and finally succeed in passing the narrow gap of 18cm with a diameter of 36 cm. H. Jia et al. previously present a quadrotor with a passively reconfigurable airframe for hybrid terrestrial locomotion[20], their vehicle pass through a narrow gap of 10 cm with a diameter of 18 cm. Compared to the vehicle, for the same diameter, Roller-Quadrotor can safely pass through a narrow gap of 9 cm in diameter of 18 cm, which is narrower.

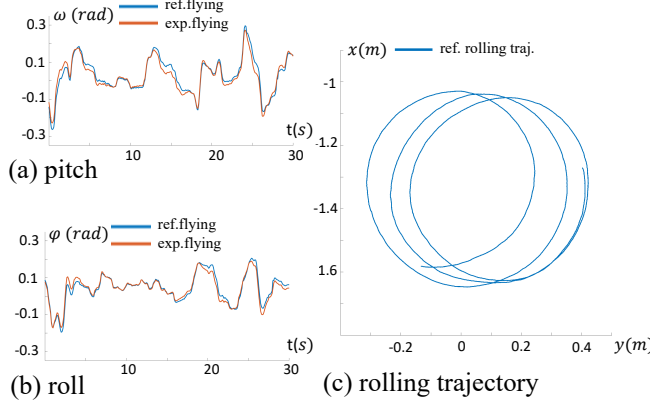


Fig. 10. (a)(b) Roll and pitch tracking during manual flight in stabilize mode in the APM flight controller. (c) Plot of vehicle rolling trajectory during ground circle rolling.

2) *Ground Circle Rolling*: We conduct the following experiments: Experiment 5.1: The experimental conditions are set as circular track radius 25 cm, clockwise (see Fig. 9) (c); Experiment 5.2: The experimental conditions are set as circular track radius 50 cm, counterclockwise (see Fig. 9 (d)). The results of Experiment 5.1 are shown as 10 (c), the vehicle rolls about 40 s. The results of Experiment 5.2 are similar.

E. Experiments of Energy Consumption

Experiment 6: We conduct the following experiments: set the rolling mode, $\omega_w = 1 \text{ rad}$ and the radius of the circular trajectory to 25 cm, clockwise. Kalantari previously presented a quadrotor named HyTAQ[7][8], adding a rolling cage to the quadrotor that makes terrestrial locomotion possible. The energy consumption experiments results are presented in Table I, these can reflect the excellent energy-saving ability of Roller-Quadrotor. The weight of Roller-Quadrotor is 1.5 kg, and the HyTAQ is 0.45 kg.

In terms of rolling energy consumption, it can roll a distance nearly 3.8 times as much as flying or operate about 42.2 times as long as flying. Compared to HyTAQ, the operating time of Roller-Quadrotor is approximately 4.7 times as lengthy as HyTAQ rolling while the rolling distance is shorter than HyTAQ, with the same vehicle mass.

F. Experiments of Hybrid Trrestrial and Aerial

Experiment 7: We conduct some comprehensive experiments, including rolling, transition from rolling to flight, take-off and flight in one experiment (see Fig. ref:Fig:introduction). The vehicle starts in rolling mode, rolling in a clockwise circle with the desired diameter of 50 cm, switches from rolling to flight mode, and finally takes off and flies.

The experiment is to simulate wheeled ground movement encountered obstacles, the vehicle can be converted into flight mode, flying over the obstacles, which solves the obstacle avoidance challenge faced by terrestrial robots.

TABLE I
RESULTS OF ENERGY CONSUMPTION EXPERIMENTS

	Experiment Situation Time Distance	Total Energy Consumption	Average Energy Consumption Per Unit kg
Roller-Quadrotor Group 1	Rolling 48 min 518.4 m	1270 mah 14.8 V	15.7 W 87.0 J/m
Roller-Quadrotor Group 2	Rolling 40.33 min 435.6 m	1060 mah 14.8 V	15.6 W 86.4 J/m
Average of Group 1 and 2	/	/	15.6 W 86.7 J/m
Roller-Quadrotor Group 3	Manual flying about 1.8 min 216 m	2000 mah 14.8 V	657.8 W 328.9 J/m
HyTAQ	Rolling 27 min 2400 m	1350 mah 11.1 V	74.0 W 50.0 J/m

V. CONCLUSION

Roller-Quadrotor is a novel hybrid aerial and terrestrial quadrotor that combines the agility of a quadrotor with the endurance of a ground vehicle. This work presents the design, modeling, and experimental validation of Roller-Quadrotor. The quadrotor uses four actuators for flight, while a unicycle-driven and rotor-assisted turning structure enables terrestrial locomotion and allows the vehicle to roll through narrow gaps. This design overcomes challenges faced by traditional rotorcraft, extending operation time and facilitating passage through narrow gaps. It also solves problems in terrestrial robots by avoiding obstacles through flight. The vehicle can switch between aerial and terrestrial locomotion and safely navigate gaps half of its diameter. In the energy consumption aspect, it can roll approximately 3.8 times farther than it can fly or operate about 42.2 times longer than it can fly. These results demonstrate the feasibility and effectiveness of Roller-Quadrotor in terms of energy conservation and terrain adaptability, particularly for rolling through narrow gaps.

In our future work, we plan to focus on improving the accuracy of models and developing advanced control algorithms, which will increase the success rate of the modal transitions and make them smoother, it can also improve the trajectory tracking accuracy. We are also considering structural optimization and weight reduction, to further improve the energy consumption performance. Furthermore, we will use planning algorithms[21] to enhance vehicle mobility.

VI. ACKNOWLEDGMENT

This work was supported in part by the Key R&D Program of Zhejiang Province under Grant 2023C01070 and 2021C01065, the National Natural Science Foundation of China under Grant 52175032, and Robotics Institute of Zhejiang University under Grant K12107 and K11805. The authors would like to thank Miss Yuhua Zhou for her help in paper writing. The authors also sincerely appreciate the valuable comments and suggestions from reviewers.

REFERENCES

- [1] Tian Y, Liu K, Ok K, et al. "Search and rescue under the forest canopy using multiple UAVs," in *The International Journal of Robotics Research*, 2020;39(10-11):1201-1221.
- [2] Abeywickrama H V , Jayawickrama B A , Ying H , et al. "Comprehensive Energy Consumption Model for Unmanned Aerial Vehicles, Based on Empirical Studies of Battery Performance," in *IEEE Access*, 2018, PP(99):1-1.
- [3] Lee T, "Collision avoidance for quadrotor UAVs transporting a payload via Voronoi tessellation," in *American Control Conference. IEEE*, 2015:1842-1848.
- [4] Zhang R, Wu Y, Zhang L, et al., "Autonomous and adaptive navigation for terrestrial-aerial bimodal vehicles," in *IEEE Robotics and Automation Letters*, 2022, 7(2): 3008-3015.
- [5] Pimentel M, Basiri M, "A bimodal rolling-flying robot for micro level inspection of flat and inclined surfaces," in *IEEE Robotics and Automation Letters*, 2022, 7(2): 5135-5142.
- [6] Page J R, Pounds P E I, "The Quadroller: Modeling of a UAV/UGV hybrid quadrotor," in *2014 IEEE/RSJ International Conference on Intelligent Robots and Systems. IEEE*, 2014: 4834-4841.
- [7] A. Kalantari and M. Spenko, "Design and experimental validation of HyTAQ, a Hybrid Terrestrial and Aerial Quadrotor," in *2013 IEEE International Conference on Robotics and Automation (ICRA)*, 2013, pp. 4445-4450.
- [8] A. Kalantari and M. Spenko, "Modeling and Performance Assessment of the HyTAQ, a Hybrid Terrestrial/Aerial Quadrotor," in *IEEE Transactions on Robotics*, vol. 30, no. 5, pp. 1278-1285, Oct. 2014.
- [9] Dudley C J, Woods A C, Leang K K, "A micro spherical rolling and flying robot," in *2015 IEEE/RSJ International Conference on Intelligent Robots and Systems (IROS)*, 2015, pp. 5863-5869.
- [10] Matus-Vargas, A., Rodriguez-Gomez, G. & Martinez-Carranza, J., "Ground effect on rotorcraft unmanned aerial vehicles: a review," in *Intel Serv Robotics* 14, 99-118 (2021).
- [11] Falanga D, Kleber K, Mintchev S, et al., "The foldable drone: A morphing quadrotor that can squeeze and fly," in *IEEE Robotics and Automation Letters*, 2018, 4(2): 209-216.
- [12] Yang T, Zhang Y, Li P, et al., "Sniae-sse deformation mechanism enabled scalable multicopter: Design, modeling and flight performance validation," in *2020 IEEE International Conference on Robotics and Automation (ICRA)*, 2020, pp. 864-870.
- [13] Yang D, Mishra S, Aukes D M, et al., "Design, planning, and control of an origami-inspired foldable quadrotor," in *2019 American Control Conference (ACC)*, 2019, pp. 2551-2556.
- [14] Fabris A, Kleber K, Falanga D, et al., "Geometry-aware compensation scheme for morphing drones," in *2021 IEEE International Conference on Robotics and Automation (ICRA)*, 2021, pp. 592-598.
- [15] Bucki N, Mueller M W, "Design and control of a passively morphing quadcopter," in *2019 International Conference on Robotics and Automation (ICRA)*, 2019, pp. 9116-9122.
- [16] Pathak, K. , J. Franch , and S. K. Agrawal. "Velocity and position control of a wheeled inverted pendulum by partial feedback linearization," in *IEEE Trans Robotics*, 21.3(2005):505-513.
- [17] Wu, C. S. , Z. Y. Chiu , and J. S. Liu . "Time-Optimal Trajectory Planning along Parametric Polynomial Lane-Change Curves with Bounded Velocity and Acceleration: Simulations for a Unicycle Based on Numerical Integration." in *Modelling and Simulation in Engineering* 2018(2018):1-19.
- [18] W. Dong, G. -Y. Gu, Ye Ding, X. Zhu and H. Ding, "Ball juggling with an under-actuated flying robot," in *2015 IEEE/RSJ International Conference on Intelligent Robots and Systems (IROS)*, 2015, pp. 68-73.
- [19] M. W. Mueller, M. Hehn and R. D'Andrea, "A computationally efficient algorithm for state-to-state quadrocopter trajectory generation and feasibility verification," in *2013 IEEE/RSJ International Conference on Intelligent Robots and Systems (IROS)*, 2013, pp. 3480-3486.
- [20] H. Jia et al., "A Quadrotor With a Passively Reconfigurable Airframe for Hybrid Terrestrial Locomotion," in *IEEE/ASME Transactions on Mechatronics*, vol. 27, no. 6, pp. 4741-4751, Dec. 2022.
- [21] Yu, Huan et al., "Catch Planner: Catching High-Speed Targets in the Flight." in *arXiv preprint arXiv:2302.04387*, 2023.